⌘ *Author's Choice*

THE JOURNAL OF BIOLOGICAL CHEMISTRY VOL. 285, NO. 47, pp. 36977–36983, November 19, 2010

The Streptococcal Binding Site in the Gelatin-binding Domain of Fibronectin Is Consistent with a Non-linear Arrangement of Modules*

Received for publication, June 22, 2010, and in revised form, August 13, 2010 Published, JBC Papers in Press, September 15, 2010, DOI 10.1074/jbc.M110.156935

Kate E. Atkin[‡1,2], Andrew S. Brentnall[‡1,2], Gemma Harris[‡2], Richard J. Bingham[‡3], Michele C. Erat[§4], Christopher J. Millard[§], Ulrich Schwarz-Linek[¶], David Staunton[§], Ioannis Vakonakis[§5], Iain D. Campbell[§], and Jennifer R. Potts[‡‖2,6]

From the Departments of [‡]Biology and [‖]Chemistry, University of York, Heslington, York, YO10 5DD, United Kingdom, the [§]Department of Biochemistry, University of Oxford, Oxford OX1 3QU, United Kingdom, and the [¶]Centre for Biomolecular Sciences, University of St. Andrews, North Haugh, St. Andrews, Fife KY16 9ST, Scotland, United Kingdom

Fibronectin-binding proteins (FnBPs) of *Staphylococcus aureus* and *Streptococcus pyogenes* mediate invasion of human endothelial and epithelial cells in a process likely to aid the persistence and/or dissemination of infection. In addition to binding sites for the N-terminal domain (NTD) of fibronectin (Fn), a number of streptococcal FnBPs also contain an upstream region (UR) that is closely associated with an NTD-binding region; UR binds to the adjacent gelatin-binding domain (GBD) of Fn. Previously, UR was shown to be required for efficient streptococcal invasion of epithelial cells. Here we show, using a *Streptococcus zooepidemicus* FnBP, that the UR-binding site in GBD resides largely in the ^{8}F1^{9}F1 module pair. We also show that UR inhibits binding of a peptide from the α1 chain of type I collagen to ^{8}F1^{9}F1 and that UR binding to ^{8}F1 is likely to occur through anti-parallel β-zipper formation. Thus, we propose that streptococcal proteins that contain adjacent NTD- and GBD-binding sites form a highly unusual extended tandem β-zipper that spans the two domains and mediates high affinity binding to Fn through a large intermolecular interface. The proximity of the UR- and NTD-binding sequences in streptococcal FnBPs is consistent with a non-linear arrangement of modules in the tertiary structure of the GBD of Fn.

Many cell surface-anchored bacterial proteins bind extracellular matrix proteins in the host. These proteins, also known as MSCRAMMs (microbial surface components recognizing adhesive matrix molecules) (1, 2), are likely to play roles in the establishment, dissemination, and/or persistence of infection by mediating interactions with host tissues. Fibronectin (Fn)[7]-binding proteins (FnBPs) from *Staphylococcus aureus* (FnBPA/FnBPB) (3) and *Streptococcus pyogenes* (SfbI/F1) (4) mediate adhesion to and invasion of host cells (5–9), including endothelial and epithelial cells. Fn is a large glycoprotein of ~230 kDa (monomer molecular mass) which is present in human plasma in a soluble, dimeric form and in the extracellular matrix in an insoluble form. Fn has a modular structure, composed of type 1, type 2, and type 3 (F1, F2, and F3) modules that combine to form functional domains (10, 11). The N-terminal domain (NTD) is composed of five F1 modules ($^{1-5}$F1), and the adjacent gelatin-binding domain (GBD) contains ^{6}F1^{1}F2^{2}F2$^{7\text{-}8\text{-}9}$F1 (Fig. 1*A*). FnBPs from *S. pyogenes*, *S. aureus*, *Streptococcus dysgalactiae*, and *Borrelia burgdorferi* bind to the NTD through a tandem β-zipper (12–15). In other words, within these FnBPs, intrinsically disordered NTD-binding bacterial repeats (FnBRs) contain short motifs that form an anti-parallel β-strand along the triple-stranded β-sheet of consecutive F1 modules in the NTD. Structural evidence for this unusual mechanism of protein-protein recognition has been provided by both NMR spectroscopy and x-ray crystallography for all five F1 modules of the NTD and for several bacterial peptides (12, 14). Although FnBPs from staphylococci and streptococci contain multiple FnBRs (2), BBK32 from *B. burgdorferi* appears to contain only one (15).

As is clear from its name, the GBD has long been known to bind gelatin (denatured collagen) (16). Recently, evidence for a β-zipper interaction between an F1 module of the GBD and a synthetic peptide from the α1 chain of type I collagen was obtained using both NMR spectroscopy and x-ray crystallography. A crystal structure of a GBD module pair, ^{8}F1^{9}F1, with peptide bound (17) revealed that the collagen peptide forms an anti-parallel β-strand along the C-terminal (E) strand of triple-stranded β-sheet of ^{8}F1. The GBD of Fn has also been shown to be important for binding of pathogenic bacteria to Fn. Talay *et al.* (18) showed that SfbI from *S. pyogenes* binds to both NTD and GBD. Binding to GBD is mediated through a spacer domain (also known as an upstream region (UR)) on SfbI adjacent to and upstream of the FnBR region. Cell invasion assays demonstrated that the SfbI UR and FnBR regions

* This research was supported by the BBSRC.
⌘ *Author's Choice*—Final version full access.
[1] Both authors contributed equally to this work.
[2] Supported by the British Heart Foundation.
[3] Present address: Dept. of Chemical and Biological Sciences, School of Applied Sciences, University of Huddersfield, Queensgate, Huddersfield HD1 3DH, United Kingdom.
[4] Supported by a FP7 Marie Curie Fellowship.
[5] Supported by the Wellcome Trust.
[6] To whom correspondence should be addressed: Dept. of Biology, University of York, Heslington, York YO10 5DD, United Kingdom. Tel.: 44-1904-328679; Fax: 44-1904-328825; E-mail: jp516@york.ac.uk.
[7] The abbreviations used are: Fn, fibronectin; FnBP, fibronectin-binding protein; NTD, N-terminal domain; GBD, gelatin-binding domain; FnBR, fibronectin binding repeat; UR, upstream region; ESI, electrospray ionization; ITC, isothermal calorimetry; HSQC, heteronuclear single-quantum coherence; NOESY, nuclear Overhauser effect spectroscopy; TOCSY, total correlation spectroscopy.

are both required for efficient invasion of streptococci into the eukaryotic cell (18).

It is likely that bacterial peptides, in binding Fn, harness (and probably modify) its normal physiological activity. Thus, understanding the mechanism of interaction of FnBPs with Fn will lead to a better understanding not only of the role of FnBPs in infection but also of the activities of Fn itself and how they might be controlled. For example, an *S. pyogenes* UR-containing peptide has been shown to reduce Fn matrix polymerization (19) and to increase turnover of Fn (20) and collagen I (21), suggesting possible applications in reducing pathological matrix remodeling (22).

Streptococcus zooepidemicus (*Streptococcus equi* subspecies *zooepidemicus*) is a frequent cause of opportunistic pyogenic infections in horses and also, although rarely, can cause human infections (23). An FnBP from *S. zooepidemicus*, FnZ (Fig. 1*B*), has a sequence organization similar to SfbI from *S. pyogenes* (2, 24), but the UR-like sequence lies between the first and second of five putative FnBRs (2, 24) (Fig. 1*B*). The SfbI UR motif LAGESGET is conserved in the FnZ UR (Fig. 1*C*) (24). Because a similar motif is also present in the α1(I) collagen peptide (Fig. 1*C*), we hypothesized that bacterial peptides might bind to the GBD via the same mechanism as collagen and compete with collagen for Fn binding.

The aim of this work is to determine the mechanism of binding of streptococcal FnBPs to the GBD. First, we show that a *S. zooepidemicus* FnZ peptide binds both ^{8}F1^{9}F1 and GBD. Second, data are presented that support an anti-parallel β-zipper mode of binding for FnZ to ^{8}F1^{9}F1. Last, we show that the *S. zooepidemicus* FnZ peptide inhibits binding of the collagen peptide to ^{8}F1^{9}F1, presumably due to overlap of the binding sites on ^{8}F1^{9}F1. The role of conserved residues in ^{8}F1-binding motifs and the consequences of the proximity of the NTD- and GBD-binding sites in the streptococcal proteins for the structure of Fn are also discussed.

EXPERIMENTAL PROCEDURES

Expression and Purification of Recombinant ^{8}F1^{9}F1—Unlabeled and uniformly ^{15}N-labeled ^{8}F1^{9}F1 module pair (Fn precursor residues 516–608) was expressed in *Pichia pastoris* using a procedure similar to that described previously (25). Secreted protein was concentrated from fermentation media by cation exchange chromatography on a 5-ml SP-Sepharose Fast Flow column (GE Healthcare) at pH 3.0, eluting with a gradient from 0 to 1 M NaCl in 20 mM citric acid over 50 column volumes. Fractions containing protein were incubated with Endo *Hf* (New England Biolabs) at pH 5.5 to trim the sugars attached to glycosylation sites at Asn^{528} and Asn^{542} back to a single GlcNAc. ^{8}F1^{9}F1 was further purified by gelatin affinity chromatography on an XK16 column (GE Healthcare) packed with 20 ml of gelatin-Sepharose 4B (GE Healthcare). Protein was loaded in phosphate-buffered saline (PBS) at pH 7.3 at 4 °C and eluted with a gradient from 0 to 4 M urea. The protein was finally purified by size exclusion chromatography on a HiLoad Superdex 75 gel filtration column (GE Healthcare) equilibrated in 40 mM NaH_2PO_4/K_2HPO_4, pH 7.3, 150 mM NaCl. The ^{8}F1^{9}F1 concentration was determined from absorbance at 280 nm, and the molecular weight was confirmed by electrospray ionization mass spectrometry (ESI-MS). SDS-PAGE analysis of the purified protein showed a single band.

Expression and Purification of FnZ—DNA for residues 370–428 of FnZ from *S. zooepidemicus* (24) was produced synthetically (Entelechon) and cloned into a pGEX-6P-1 vector (GE Healthcare). The protein was expressed recombinantly in *E. coli* BL21 (DE3) as a GST-tagged fusion protein using autoinduction. The fusion was isolated from soluble bacterial cell lysates using a 5-ml GSTrap high performance column (GE Healthcare) equilibrated in PBS, pH 7.3, and eluted using 20 mM Tris-HCl, 50 mM NaCl, 10 mM reduced glutathione, pH 7.0. Appropriate fractions were pooled, and the glutathione was removed using dialysis. After cleavage of the affinity tag using 3C protease (Novagen) (leaving five vector residues, GPLGS, at the N terminus), the FnZ construct was further purified using reversed phase high performance liquid chromatography on a C4 Jupiter column (Phenomenex). Buffer A was 0.15% trifluoroacectic acid (TFA), and buffer B was 100% acetonitrile, 0.1% TFA. Protein was loaded onto the column equilibrated in 10% buffer B and eluted on a continuous linear gradient of 10–45% buffer B in 50 ml, and appropriate fractions were lyophilized. Concentration measurements were made based on mass, and the molecular weight was confirmed by ESI-MS.

Preparation of Fn Fragments and Synthetic Peptides—The GBD of Fn was obtained as a lyophilized proteolytic fragment (Sigma) and dialyzed into 10 mM NaH_2PO_4/K_2HPO_4 (pH 7.3) before use. A recombinant Fn 100-kDa N-terminal fragment (Fig. 1*A*) was expressed and purified as described elsewhere (26) and dialyzed against PBS (pH 7.3) prior to use. The *S. zooepidemicus* FnZ synthetic peptides (sequences RNPHLMGIGGGLAGESGETTPK and LAGESGET) were obtained from Alta Bioscience UK. The N and C termini of the shorter peptide were capped by acetylation and amidation, respectively; the termini of the longer peptide were uncapped. Peptide concentration measurements were made based on mass.

Isothermal Titration Calorimetry (ITC)—ITC experiments were carried out using a VP-ITC microcalorimeter (MicroCal Inc., Northampton, MA). In a typical experiment, the cell contained 1.4 ml of Fn fragment (^{8}F1^{9}F1, GBD, or 100 kDa), and the syringe contained 277 μl of FnZ (synthetic peptide or recombinant protein) at a concentration 10–20 times higher than that of the protein in the cell. If possible, the cell concentration was chosen to correspond to a c value of 100–1000, where c = [protein]/predicted K_d (27). Titrations with ^{8}F1^{9}F1 and GBD were carried out in 10 mM NaH_2PO_4/K_2HPO_4, pH 7.4, at 25 °C. Both the cell and syringe solutions were degassed at 20 °C for 15 min before use. Both sets of titrations were carried out as follows. One preinjection of 2 μl of syringe solution was followed by 39 injections of 7 μl at an injection speed of 0.5 μl/s. Stirring speed was 307 rpm, and there was a delay of 360 s between injections. For both titrations, a separate heat of dilution experiment was performed by injecting peptide into buffer. The averaged heats of dilution were subtracted from the main experiments. The titration with the 100-kDa Fn frag-

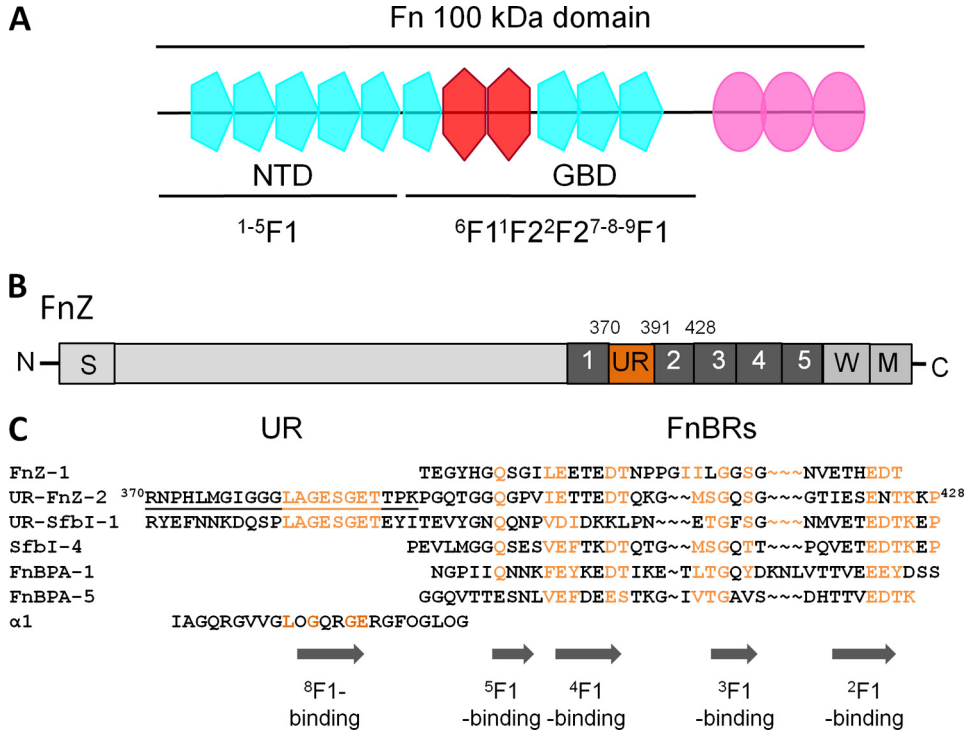

FIGURE 1. **FnZ and Fn.** *A*, schematic of the 100-kDa N-terminal region of Fn showing F1 (*blue*), F2 (*red*), and F3 (*pink*) modules and showing the location of the NTD and GBD. *B*, schematic representation of FnZ showing putative functional domains. *S*, a signal sequence. Putative FnBRs (*R1–R5*) are *colored dark gray*, and the UR region is shown in *orange*. *M* and *W*, membrane- and wall-spanning regions, respectively. *C*, sequence alignment of putative ^{8}F1^{9}F1/GBD binding (UR) and NTD-binding regions (FnBRs) from streptococcal and staphylococcal FnBPs and from the α1 chain of type I collagen. Residue numbers are given for FnZ, conserved residues in FnBRs and UR are *highlighted* in *orange*, and the location of F1-binding motifs based on published data is indicated. The FnZ peptide used in this study is *underlined*. Hydroxyproline residues in the collagen peptide are indicated with an *O*.

ment was performed at 37 °C in PBS (pH 7.3) after degassing both cell and syringe solutions at 30 °C for 15 min. One preinjection of 2 μl of syringe solution was followed by 26 injections of 5 μl at an injection speed of 0.5 μl/s. Stirring speed was 302 rpm, and there was a delay of 300 s between injections. The heat of dilution was taken as the average heat of six points at the end of the titration. Data were analyzed using MicroCal Origin software (version 7), with data being fitted to a one-site binding model.

NMR Spectroscopy—All experiments were carried out at 25 °C on a Bruker Avance 700-MHz spectrometer. Samples were prepared by dissolving uniformly labeled ^{15}N-^{8}F1^{9}F1 to a concentration of 0.2 and 1.0 mM, for binding studies and confirmation of previous ^{8}F1^{9}F1 assignments (25), respectively, in 90% H_2O, 10% D_2O containing 150 mM NaCl, 20 mM KH_2PO_4/Na_2HPO_4, 0.02% sodium azide with pH adjusted to 7.2. A series of heteronuclear single-quantum coherence (HSQC) experiments with excitation sculpting for solvent suppression and with sensitivity enhancement (28) were carried out with increasing concentrations of synthetic FnZ and LAGESGET peptides (0.05, 0.1, 0.15, 0.2, 1.0, 1.5, and 2.0 mol eq) for binding studies; three-dimensional ^{1}H^{15}N-HSQC-NOESY and ^{1}H^{15}N-HSQC-TOCSY experiments were employed for spectral assignment. HSQC peaks for most ^{8}F1^{9}F1 residues were assigned *de novo* in both free and FnZ peptide-bound spectra, but for five peaks that were very weak in the spectra of the ^{8}F1^{9}F1-peptide complex, assignments were based on assignments of the ^{8}F1^{9}F1-collagen peptide complex (17) (BMRB entry 15986). Data processing and referencing were performed using NMRPipe (29), and spectral assignment was performed with CCPNMR Analysis version 1.0.15 (30).

Competition Experiment—Competition between the FnZ peptide and the collagen peptide for binding to ^{8}F1^{9}F1 was demonstrated by fluorescence anisotropy measurements. Samples contained a 50 nM concentration (determined by absorbance at 280 nm) of an N-terminally 5-carboxyfluorescein-labeled α1(I) collagen peptide spanning residues 778–799, which has been shown to bind ^{8}F1^{9}F1 with an affinity (K_d) of 4.5 μM (17); unlabeled ^{8}F1^{9}F1 at concentrations of 10, 20, or 30 mM; and unlabeled FnZ peptide at increasing concentrations in a 20 mM Tris-HCl (pH 7.4), 150 mM NaCl buffer. Samples were excited at 485 nm with a 515 nm cut-off, and fluorescence was observed at 538 nm using an M5 fluorometer (Molecular Devices) at 25 °C. Differences in fluorescence anisotropy (F_A) were simultaneously fit for all ^{8}F1^{9}F1 concentrations using the formula,

$$F_A = F_{A,\text{final}} + dF_A\left(\frac{[P] - 0.5a}{K_{dBL} + [P] - 0.5a}\right) \quad \text{(Eq. 1)}$$

where

$$a = [P] + [CL] + K_{dCL} - \sqrt{([P] + [CL] + K_{dCL})^2 - 4[P][CL]} \quad \text{(Eq. 2)}$$

where F_A is the fluorescence anisotropy measured at each point, $F_{A,\text{final}}$ is the fluorescence anisotropy at saturation of competing ligand (FnZ peptide), [P] is the protein (^{8}F1^{9}F1) concentration, [CL] is the concentration of competing ligand, K_{dCL} is the affinity of the competing ligand, and K_{dBL} is the affinity of bound ligand (collagen peptide, 4.5 μM).

RESULTS

FnZ Binds the 100-kDa N-terminal Region of Fn with High Affinity—Residues 370–428 of FnZ contains a site with high sequence homology to NTD-binding FnBRs from *S. pyogenes* and *S. aureus* (2) and to the GBD-binding UR region of SfbI from *S. pyogenes* (18, 24) (Fig. 1*C*). ITC (Fig. 2*A* and Table 1) shows that FnZ(370–428) binds a recombinant 100-kDa N-terminal fragment of Fn containing both the NTD and GBD (in addition to three F3 modules; Fig. 1*A*) (26) with high affinity (K_d 0.8 ± 0.1 nM).

The UR/spacer of FnZ binds ^{8}F1^{9}F1—A sequence alignment of the UR sequences of FnZ and SfbI with the collagen I α1 peptide (residues 778–799; Fig. 1*C*) shows that the LAGESGET motif is conserved between FnZ and SfbI and has some homology with the collagen peptide. ITC experiments (Fig. 2 and Table 1) show that the peptide spanning residues 370–391 from FnZ (Fig. 1*C*) binds with micromolar affinity to both the GBD (K_d of 0.54 ± 0.04 μM; Fig. 2*B*) and ^{8}F1^{9}F1 (K_d of 10.9 ± 0.3 μM; Fig. 2*C*). The relative affinities suggest that the majority of the FnZ peptide binding site is within ^{8}F1^{9}F1, with some limited involvement (through direct binding or through stabilizing interdomain interfaces) of other residues in GBD.

FnZ Residues 370–391 Bind to ^{8}F1 via an Anti-parallel β-Zipper—The interaction between ^{8}F1^{9}F1 and the FnZ peptide was explored using NMR spectroscopy; a series of ^{1}H^{15}N-HSQC spectra were acquired for uniformly ^{15}N-labeled ^{8}F1^{9}F1 with increasing concentrations of peptide (Fig. 3*A*). The ^{1}H^{15}N-HSQC spectrum of ^{8}F1^{9}F1 when bound to the FnZ peptide was assigned using three-dimensional ^{1}H^{15}N-HSQC-NOESY and ^{1}H^{15}N-HSQC-TOCSY experiments. A plot of chemical shift changes between the free and bound forms of ^{8}F1^{9}F1 (Fig. 3*B*) shows that the most significant differences occur in the E-strand of ^{8}F1 (Fig. 3*C*). Chemical shift changes were also observed in the A-strand of ^{9}F1. In addition, four residues in the D-E loop of ^{9}F1 could be assigned in the bound form, due to a sharpening of resonances compared with spectra of the unbound form of ^{8}F1^{9}F1, where their assignment was not possible. This suggests that in the unbound form, this loop undergoes conformational exchange, resulting in line broadening that is reduced upon peptide binding. *S. aureus* and *S. pyogenes* FnBRs and the collagen α1(I) peptide bind along the E-strand of their respective F1 modules in an anti-parallel orientation. Fig. 3, *A* and *B*, shows that a shorter peptide (LAGESGET), from the C terminus of the FnZ ^{8}F1^{9}F1-binding peptide, has no affect on ^{9}F1 residues (*e.g.* Tyr^{585} and Cys^{587}) that underwent chemical shift changes upon the addition of the longer peptide. Because ^{8}F1 residues (*e.g.* Asn^{542} and Glu^{536}) are affected by binding of both peptides, it is clear that FnZ also binds ^{8}F1^{9}F1 in an anti-parallel orientation.

The FnZ Peptide Binds Competitively to the Collagen-binding Site of ^{8}F1^{9}F1—The ability of the FnZ peptide to compete with the collagen peptide for ^{8}F1^{9}F1 binding was tested by fluorescence anisotropy. Fig. 4 shows that increasing concentrations of unlabeled FnZ peptide added to ^{8}F1^{9}F1 plus fluorescently labeled collagen peptide led to a steady decrease in anisotropy, suggesting dissociation of the collagen peptide-^{8}F1^{9}F1 complex. The K_d of FnZ peptide binding was determined from this experiment to be 1.9 ± 0.1 μM, indicating tighter binding to ^{8}F1^{9}F1 than observed for the collagen peptide under similar conditions by fluorescence anisotropy (4.5 μM) (17). Together, these results suggest that residues 370–391 from FnZ bind to the same region of ^{8}F1^{9}F1 as the collagen peptide and through a similar anti-parallel β-zipper mechanism.

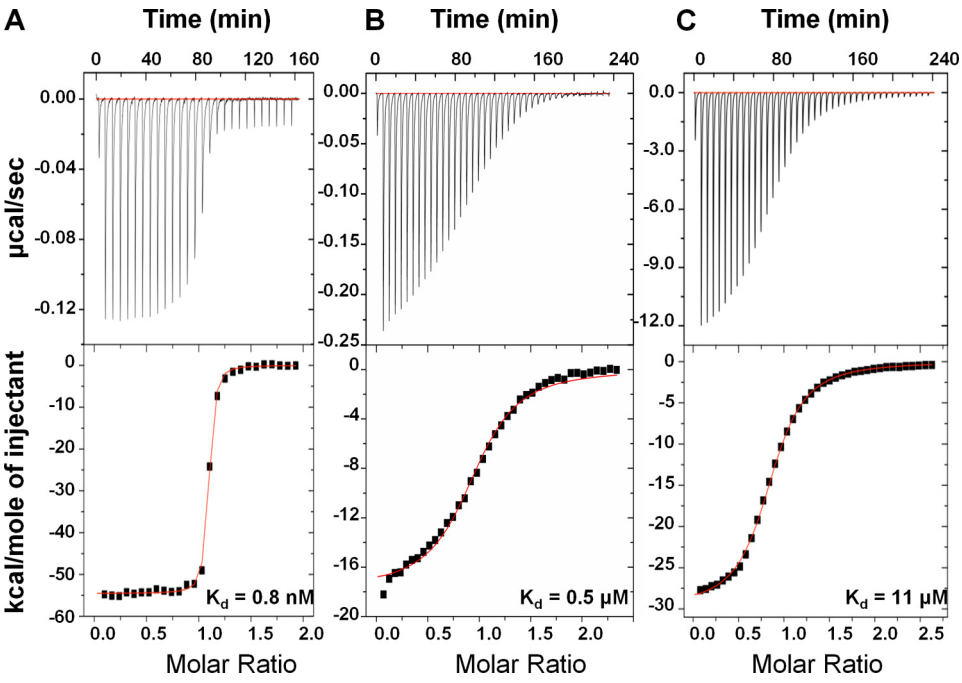

FIGURE 2. **ITC of FnZ binding to Fn domains.** The binding isotherms for FnZ(370–428) with the 100-kDa fragment (*A*) and the interaction of FnZ peptide 370–391 with GBD (*B*) and ^{8}F1^{9}F1 (*C*) are shown. The *top panels* show the heat differences upon injection of peptide, and the *lower panels* show the integrated heats of injection, with the best fit to a one-site binding model using MicroCal Origin. Thermodynamic parameters for these experiments are summarized in Table 1.

DISCUSSION

UR sequences are found in FnBPs from pathogenic streptococci (2, 18) and in BBK32, an FnBP from *B. burgdorferi* (2, 31). The UR binding site in SfbI from *S. pyogenes* had

TABLE 1

ITC analysis of interactions of FnZ with Fn domains

Thermodynamic parameters for the interaction of FnZ peptide with ^{8}F1^{9}F1 and GBD and of FnZ(370–428) with the 100-kDa Fn fragment. Errors are from the curve fitting.

Fn domain	[FnZ peptide]	[Fn domain]	Δ*H*	Δ*S*	K_d	*n*
	mM	mM	kcal/mol	cal/mol K^{-1}	μM	
^{8}F1^{9}F1	2.97	0.24	−29.8	−77.2	10.9 ± 0.3	0.86
GBD	0.11	0.01	−17.7	−30.8	0.54 ± 0.04	0.96
	[FnZ(370–428)]	[Fn domain]	Δ*H*	Δ*S*	K_d	*n*
	mM	mM	kcal/mol	cal/mol K^{-1}	μM	
100 kDa	0.020	0.001	−54.6	−134.0	0.0008 ± 0.0001	1.06

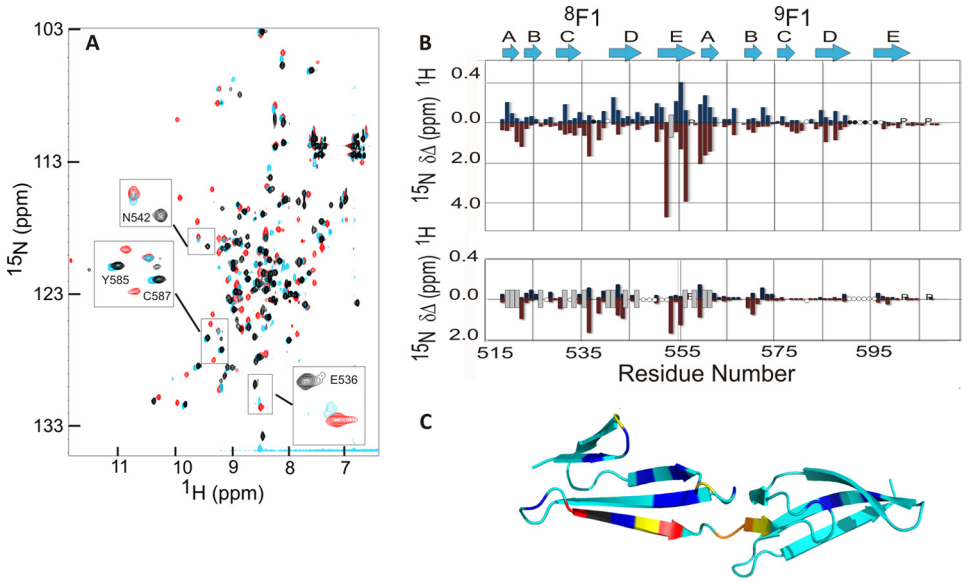

FIGURE 3. **Identification of the FnZ peptide binding site and binding orientation on ^{8}F1^{9}F1 using NMR spectroscopy.** *A*, overlay of the ^{1}H^{15}N HSQC spectra of free ^{8}F1^{9}F1 (*black*) and of ^{8}F1^{9}F1 bound to the FnZ (*red*) and LAGESGET (*cyan*) peptides. *Highlighted residues* are mentioned under "Results." *B*, chemical shift perturbation map for ^{15}N-labeled ^{8}F1^{9}F1 upon binding to the FnZ (*top*) and LAGESGET (*bottom*) peptides. *Blue* and *red bars* indicate absolute chemical shift differences in backbone amide ^{1}H and ^{15}N nuclei, respectively, between free and peptide-bound ^{8}F1^{9}F1. *P*, proline residues; ○, unassigned residues; ●, residues previously unassigned but now identified. The approximate location of previously defined secondary structure elements of the F1 modules are shown above. Peaks that disappear upon peptide binding from their chemical shift in free ^{8}F1^{9}F1 but cannot be assigned in the peptide-bound spectrum are indicated by a *gray bar* of arbitrary size. *C*, location of combined chemical shift perturbations (square root of $(\Delta\delta_{HN}^2 + 0.2\Delta\delta_N^2)$) on FnZ peptide binding mapped onto the structure of ^{8}F1^{9}F1 (17) (Protein Data Bank entry 3EJH). Small to large chemical shift changes are indicated by as follows: *cyan* < *blue* < *yellow* < *orange* < *red* and Trp^{553} (*gray*; prepared using PyMOL) (35).

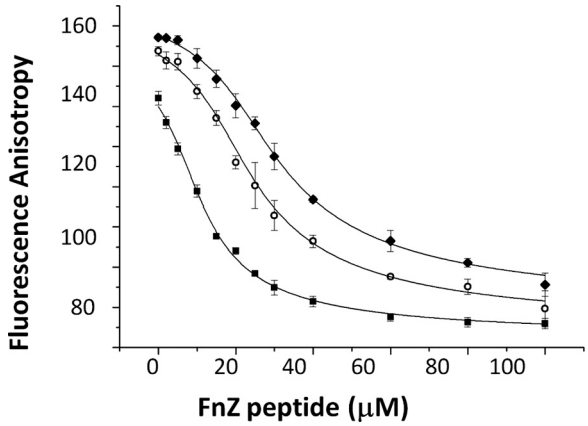

FIGURE 4. **Competitive binding of FnZ peptide to ^{8}F1^{9}F1 in presence of collagen peptide, demonstrated by fluorescence anisotropy measurements.** Unlabeled FnZ peptide at increasing concentrations was incubated with unlabeled ^{8}F1^{9}F1 at 10 (■), 20 (○), and 30 μM (◆) and the collagen peptide labeled with 5-carboxyfluorescein. Data were fit using Origin software. *Error bars* (S.D.) correspond to instrumental readout error and derive from triplicate measurements.

been located to the GBD (18). Here we localized the FnZ UR binding site within GBD by showing that it binds primarily to the ^{8}F1^{9}F1 module pair.

We were unable to determine the structure of the ^{8}F1^{9}F1-FnZ peptide complex using either NMR spectroscopy or x-ray crystallography. However, by close comparison of the UR and collagen peptide sequences with previously identified F1-binding motifs from *S. aureus* and *S. pyogenes* FnBRs and the available F1 module-peptide structures (Fig. 5), it is possible to understand the role of conserved residues in the ^{8}F1-binding motif of UR. For example, the glycine residue in the GET (UR) or GER (collagen peptide) appears to be conserved to avoid a steric clash with Trp^{553} in the E-strand of ^{8}F1 (Fig. 5*A*). This is similar to the role of a conserved glycine residue in *S. aureus* FnBR ^{3}F1-binding motifs (Fig. 5*A*) (14) because the E-strand of ^{3}F1 contains a tryptophan side chain in a similar orientation to the ^{8}F1 E-strand tryptophan (Fig. 5). This E-strand tryptophan residue is not conserved in ^{2}F1, so here the equivalent peptide residue in the FnBR is the glutamate of the EDT motif (Fig. 5*B*), which forms a salt bridge with an arginine residue in the C-strand of the F1 module (Fig. 5*A*). In the collagen peptide-^{8}F1^{9}F1 structure, due to the requirement for the glycine, this interaction is shifted two residues along the peptide and is formed by the glutamine in GQR (Fig. 5*A*) and thus in UR by the glutamate in GES. In ^{3}F1-binding motifs, there is no equivalent negatively charged or polar residue to interact with the C-strand arginine, and in isolation, this motif binds ^{3}F1 only very weakly (13). In ^{2}F1 binding, the aspartate of the EDT makes polar contacts with an arginine in the loop between the D and E strands. The sequence of this loop is very similar in ^{8}F1, and the glutamate in the collagen peptide GER makes a similar interaction (Fig. 5*A*) as, we suggest, does the glutamate in the GET in UR. The ^{3}F1-binding motif lacks the negatively charged residue that could interact with the lysine residue in the D-E loop of ^{3}F1. We predict that the threonine in the GET UR motif interacts with backbone atoms in the B-strand and D-E loop of the F1 module (as observed for homologous hydroxyl-containing residues in ^{2}F1- and ^{4}F1-binding motifs from *S. aureus* FnBPA (14)). The leucine in the LAG (UR) sequence is likely to be involved in hydrophobic contacts similar to those previously observed for the leucine in the LPG sequence in the collagen peptide (17). The role of the glycine in these motifs is less clear and will require further investigation.

These findings have important implications for the structure of the GBD. Fig. 6 shows a model of the 70-kDa region of Fn that contains both the NTD and GBD and the sequence of UR FnZ-2 (Fig. 1*C*). The binding sites for F1 modules in the FnZ sequence are indicated, based on our previous work studying homologous proteins from *S. pyogenes* (12) (13) and *S. aureus* (14) and on the work presented here. What is immediately striking is that there are only four residues between the most N-terminal ^{5}F1-binding residue and the most C-terminal ^{8}F1-binding residue based on crystal structures of *S. aureus* FnBPA-1 and FnBPA-5 peptides in complex with ^{4}F1^{5}F1 (14) and on the

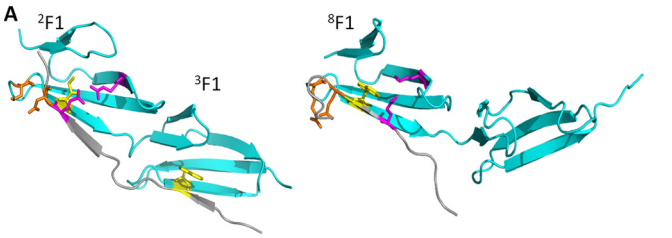

B

^{2}F1 ^{95}ETCFDKYTGNTYRVGDTYERPKD~~SMIWDCTCIGAGRGRISCTIA^{138}
^{3}F1 ^{139}NRCHEGG~~QSYKIGDTWRRPHETGGYMLECVCLGNGKGEWTCKPI^{182}
^{8}F1 ^{516}DQCIVDD~~ITYNVNDTFHKRHE~EGHMLNCTCFGQGRGRQKCDPVD^{599}

^{2}F1-binding FnBPA-1	^{540}VTTVEEEY^{547}
^{2}F1-binding FnBPA-5	^{664}DHTTVEDT^{671}
Collagen (^{8}F1-binding)	^{784}LOGQRGER^{792}
FnZ/SfbI UR (^{8}F1-binding)	^{381}LAGESQET^{388}
^{3}F1-binding FnBPA-1	^{530}TLTQQY^{535}
^{3}F1-binding FnBPA-5	^{657}IVTQAV^{662}

FIGURE 5. **Comparison of F1-binding motifs and the role of conserved residues.** *A*, structure of ^{2}F1^{3}F1 in complex with the ^{2}F1^{3}F1-binding motif from FnBPA-5 of *S. aureus* FnBPA (14) (Protein Data Bank entry 3CAL) and of ^{8}F1^{9}F1 in complex with the peptide from the α1 chain of type I collagen (17) (Protein Data Bank entry 3EJH). Conserved side chains mentioned under "Results" are shown. *B*, sequence alignments of ^{2}F1, ^{3}F1, and ^{8}F1 and of F1-binding motifs. *Coloring* of *side chains* is as in *A*. Sequence numbering is according to UniProtKB accession codes P02751 (fibronectin), P14738 (FnBPA), P72416 (FnZ), and P02452 (collagen α1(I) chain after subtraction of signal and propeptide sequences).

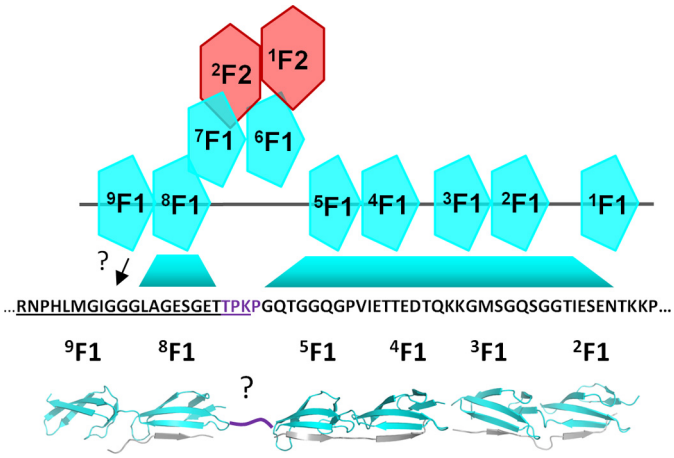

FIGURE 6. **Model of the 70-kDa (NTD + GBD) domain of Fn in complex with FnZ(370–428) highlighting the unusual extended tandem β-zipper proposed to form across NTD and GBD.** The locations of F1-binding motifs in FnZ based on previous data from SfbI-Fn and FnBPA-Fn interactions and from data in the current work are indicated. The *question marks* indicate that the location of the binding site on ^{9}F1 is uncertain, as is the conformation of the four residues (*purple*) between the ^{5}F1 and ^{8}F1-binding motifs. The model was assembled from Protein Data Bank entries 3CAL, 2RLO (14), and 3EJH (17).

^{8}F1^{9}F1-collagen peptide complex (17). Thus, as suggested previously by the hairpin arrangement of modules in the solution structure of ^{6}F1^{1}F2^{2}F2 (32), the GBD modules appear to have a non-linear arrangement in the complex. In fact, the FnZ sequence suggests that the 70-kDa (NTD + GBD) fragment of Fn presents a surface that is largely composed of F1 modules from both the NTD and GBD and that streptococcal FnBPs bind across this surface through a highly extended tandem β-zipper, forming a large protein-protein interface.

The UR region in SfbI from *S. pyogenes* is essential for efficient invasion of bacteria into epithelial cells, resulting in a 10-fold increase in invasion compared with bacteria expressing constructs that lacked this region and contained only the NTD-binding FnBRs (18). The precise molecular mechanism of this effect is unknown. We and others (15, 19) have previously suggested that the role of bacterial FnBRs in adhesion and invasion might be to disrupt intramolecular Fn-Fn interactions that maintain the compact conformation that is observed in solution, thus exposing the integrin binding site in ^{10}F3. The NTD has been implicated in such intramolecular interactions and was shown recently to interact with F3 modules (26, 33). It is less clear whether the GBD modules are involved in intramolecular interactions outside the GBD, but the high affinity and large intermolecular interface formed by FnBPs that bind both the NTD and GBD might be particularly efficient in disrupting intramolecular Fn-Fn interactions. In addition, the suggestion that IGD sequences within the GBD of Fn might bind to the αvβ3 integrin (34) means that UR binding to the GBD could have a more direct effect on the cell binding activity of Fn.

We showed (Fig. 4) that the FnZ peptide inhibited binding of a peptide from the α1 chain of type I collagen to ^{8}F1^{9}F1. Further work would be required to determine if FnBPs can inhibit intact collagen-Fn interactions. Recently, it was shown that collagen I matrix turnover is regulated by Fn (21), suggesting that the interaction between polymerized Fn and collagen stabilizes collagen within the extracellular matrix and reduces endocytosis and degradation of collagen. pUR4, a GBD/NTD-binding region from SfbI with homology to FnZ (Fig. 1*C*), inhibits Fn polymerization and enhances collagen endocytosis and degradation (21). The identification of the UR binding site within GBD and of the role of conserved residues will aid further studies of the function of the GBD in both physiological and pathological processes involving Fn and how bacterial FnBPs might modify or exploit these functions during infection.

REFERENCES

1. Joh, H. J., House-Pompeo, K., Patti, J. M., Gurusiddappa, S., and Höök, M. (1994) *Biochemistry* **33,** 6086–6092
2. Schwarz-Linek, U., Höök, M., and Potts, J. R. (2006) *Microbes Infect.* **8,** 2291–2298
3. Signäs, C., Raucci, G., Jönsson, K., Lindgren, P. E., Anantharamaiah, G. M., Höök, M., and Lindberg, M. (1989) *Proc. Natl. Acad. Sci. U.S.A.* **86,** 699–703
4. Talay, S. R., Valentin-Weigand, P., Jerlström, P. G., Timmis, K. N., and Chhatwal, G. S. (1992) *Infect. Immun.* **60,** 3837–3844
5. Peacock, S. J., Foster, T. J., Cameron, B. J., and Berendt, A. R. (1999) *Microbiology* **145,** 3477–3486
6. Massey, R. C., Kantzanou, M. N., Fowler, T., Day, N. P., Schofield, K., Wann, E. R., Berendt, A. R., Höök, M., and Peacock, S. J. (2001) *Cell Microbiol.* **3,** 839–851
7. Kintarak, S., Whawell, S. A., Speight, P. M., Packer, S., and Nair, S. P. (2004) *Infect. Immun.* **72,** 5668–5675
8. Jett, B. D., and Gilmore, M. S. (2002) *Infect. Immun.* **70,** 4697–4700
9. Ahmed, S., Meghji, S., Williams, R. J., Henderson, B., Brock, J. H., and Nair, S. P. (2001) *Infect. Immun.* **69,** 2872–2877
10. Hynes, R. (1990) *Fibronectins*, Springer-Verlag, Berlin, Germany
11. Potts, J. R., and Campbell, I. D. (1994) *Curr. Opin. Cell Biol.* **6,** 648–655
12. Schwarz-Linek, U., Werner, J. M., Pickford, A. R., Gurusiddappa, S., Kim, J. H., Pilka, E. S., Briggs, J. A., Gough, T. S., Höök, M., Campbell, I. D., and Potts, J. R. (2003) *Nature* **423,** 177–181
13. Schwarz-Linek, U., Pilka, E. S., Pickford, A. R., Kim, J. H., Höök, M., Campbell, I. D., and Potts, J. R. (2004) *J. Biol. Chem.* **279,** 39017–39025
14. Bingham, R. J., Rudiño-Piñera, E., Meenan, N. A., Schwarz-Linek, U.,

Turkenburg, J. P., Höök, M., Garman, E. F., and Potts, J. R. (2008) *Proc. Natl Acad. Sci. U.S.A.* **105,** 12254–12258
15. Raibaud, S., Schwarz-Linek, U., Kim, J. H., Jenkins, H. T., Baines, E. R., Gurusiddappa, S., Höök, M., and Potts, J. R. (2005) *J. Biol. Chem.* **280,** 18803–18809
16. Forastieri, H., and Ingham, K. C. (1985) *J. Biol. Chem.* **260,** 10546–10550
17. Erat, M. C., Slatter, D. A., Lowe, E. D., Millard, C. J., Farndale, R. W., Campbell, I. D., and Vakonakis, I. (2009) *Proc. Natl Acad. Sci. U.S.A.* **106,** 4195–4200
18. Talay, S. R., Zock, A., Rohde, M., Molinari, G., Oggioni, M., Pozzi, G., Guzman, C. A., and Chhatwal, G. S. (2000) *Cell Microbiol.* **2,** 521–535
19. Tomasini-Johansson, B. R., Kaufman, N. R., Ensenberger, M. G., Ozeri, V., Hanski, E., and Mosher, D. F. (2001) *J. Biol. Chem.* **276,** 23430–23439
20. Sottile, J., and Chandler, J. (2005) *Mol. Biol. Cell* **16,** 757–768
21. Shi, F., Harman, J., Fujiwara, K., and Sottile, J. (2010) *Am. J. Physiol. Cell Physiol.* **298,** C1265–C1275
22. Chiang, H. Y., Korshunov, V. A., Serour, A., Shi, F., and Sottile, J. (2009) *Arterioscler. Thromb. Vasc. Biol.* **29,** 1074–1079
23. Timoney, J. F. (2004) *Vet. Res.* **35,** 397–409
24. Lindmark, H., Jacobsson, K., Frykberg, L., and Guss, B. (1996) *Infect. Immun.* **64,** 3993–3999
25. Millard, C. J., Campbell, I. D., and Pickford, A. R. (2005) *FEBS Lett.* **579,** 4529–4534
26. Vakonakis, I., Staunton, D., Ellis, I. R., Sarkies, P., Flanagan, A., Schor, A. M., Schor, S. L., and Campbell, I. D. (2009) *J. Biol. Chem.* **284,** 15668–15675
27. Wiseman, T., Williston, S., Brandts, J. F., and Lin, L. N. (1989) *Anal. Biochem.* **179,** 131–137
28. Palmer, A. G., Cavanagh, J., Wright, P. E., and Rance, M. (1991) *J. Magn. Reson.* **93,** 151–170
29. Delaglio, F., Grzesiek, S., Vuister, G. W., Zhu, G., Pfeifer, J., and Bax, A. (1995) *J. Biol. NMR* **6,** 277–293
30. Vranken, W. F., Boucher, W., Stevens, T. J., Fogh, R. H., Pajon, A., Llinas, M., Ulrich, E. L., Markley, J. L., Ionides, J., and Laue, E. D. (2005) *Proteins Struct. Funct. Bioinf.* **59,** 687–696
31. Probert, W. S., Kim, J. H., Höök, M., and Johnson, B. J. (2001) *Infect. Immun.* **69,** 4129–4133
32. Pickford, A. R., Smith, S. P., Staunton, D., Boyd, J., and Campbell, I. D. (2001) *EMBO J.* **20,** 1519–1529
33. Vakonakis, I., Staunton, D., Rooney, L. M., and Campbell, I. D. (2007) *EMBO J.* **26,** 2575–2583
34. Schor, S. L., Ellis, I., Banyard, J., and Schor, A. M. (1999) *J. Cell Sci.* **112,** 3879–3888
35. Delano, W. L. (2002) *The PyMOL Molecular Graphics System*, DeLano Scientific, Palo Alto, CA